



**Fermi National Accelerator Laboratory**

**FERMILAB-Conf-90/146-E**  
[E-741/CDF]

## **Recent Results from Proton-Antiproton Colliders \***

**S. Geer**  
*Harvard University*  
*Cambridge, Massachusetts 02138*

March 1990

\* Review talk at the First International Symposium on Particles, Strings and Cosmology, Boston, Massachusetts, March 27-31, 1990.



Operated by Universities Research Association Inc. under contract with the United States Department of Energy

**Recent Results from Proton-Antiproton Colliders**

**S. Geer**

High Energy Physics Laboratory, Harvard University, 42 Oxford Street,  
Cambridge, MA 02138, USA

**ABSTRACT**

New results from the CERN and Fermilab proton-antiproton colliders are summarised. The areas covered are jet physics, direct photon production, W and Z production and decay, heavy flavor production, the search for the top quark, and the search for more exotic phenomena.

---

Review talk at the First International Symposium on Particles, Strings, and Cosmology, PASCOS-90, Northeastern University, Boston, Massachusetts, USA, March 1990.

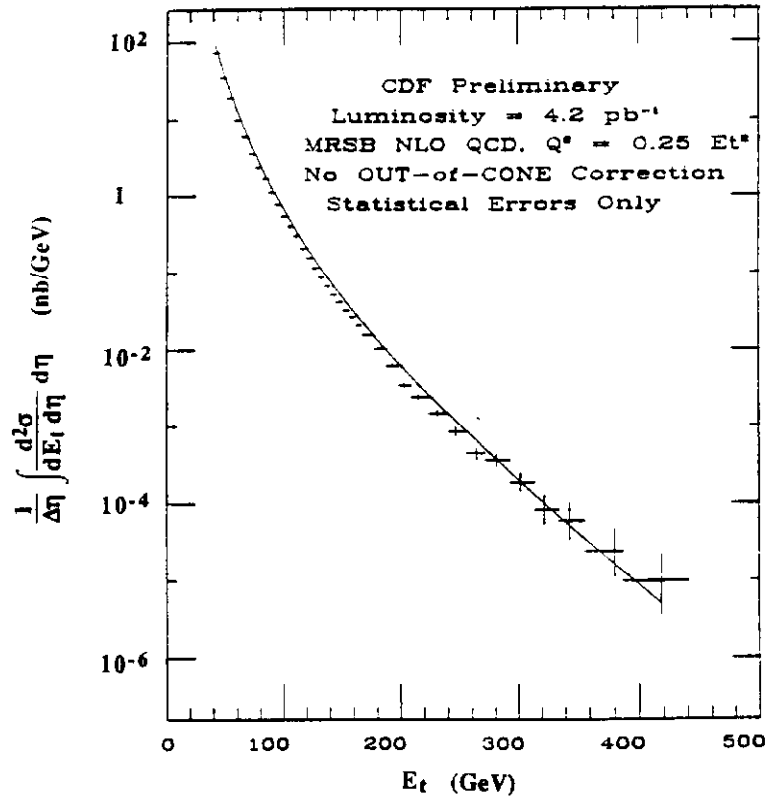


Fig. 1

Inclusive differential jet cross-section: Preliminary results from the CDF experiment are compared with the next-to-leading order QCD prediction. Jets have been reconstructed within a cone of radius  $\Delta R = 0.7$ .

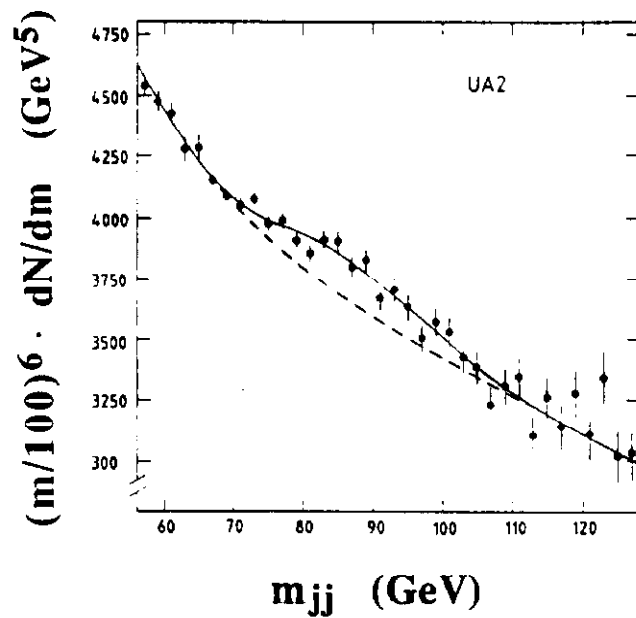


Fig. 2

Two-jet mass distribution in the neighborhood of the Intermediate Vector Bosons measured by the UA2 collaboration<sup>5</sup>. The broken line shows the background parameterization. The full line shows the best fit for signal plus background.

## 2. Jet Physics

Amongst the many new measurements of jet production at proton-antiproton colliders perhaps the most impressive are (i) the first comparison of inclusive jet production with complete next-to-leading order QCD predictions, (ii) the confirmation of the earlier UA2 observation of Intermediate Vector Boson decays into two jets, and (iii) measurements of two, three, and four jet production.

### 2.1 Inclusive Jet Production and Next-to-Leading Order QCD

In recent years the inclusive jet differential cross section has been measured both at CERN and Fermilab over intervals of jet transverse momenta ( $p_T$ ) in which the cross sections decrease by many orders of magnitude. Leading order QCD predictions for parton-parton scattering give a good description of these measurements, but unfortunately the theoretical uncertainties on the predictions arising from the uncertainties on structure functions and  $Q^2$  scale are large, typically  $\pm 50\%$ . Recently Ellis, Kunst, and Soper<sup>1</sup>, and also Aversa et al.<sup>2</sup> have used the higher order corrections to the two-to-two scattering matrix elements<sup>3</sup> to calculate the next-to-leading order predictions for inclusive jet production. The resulting predictions are compared with preliminary measurements from the CDF experiment in figure 1. The agreement is impressive. The hope is that eventually, after the experimental and theoretical systematic uncertainties have been properly evaluated, a comparison of the measured shape of the differential cross section with the theoretical predictions can be made at the  $\pm 10\%$  level. The largest uncertainties in comparing the absolute jet rates with predictions arise from the experimental uncertainties on the jet energy scale and the recorded integrated luminosity of the data samples. These uncertainties currently lead to a normalization uncertainty of about  $\pm 23\%$ .

In the future the next-to-leading order calculations for the two-jet differential cross-section should also become available, enabling two-jet mass and angular distributions to be compared with the next-to-leading order QCD predictions.

### 2.2 W and Z decays to Two Jets

The UA2 collaboration reported<sup>4</sup> the first observation of W and Z decays to two hadronic jets in 1987. Based on a data sample corresponding to an integrated luminosity of  $0.73 \text{ pb}^{-1}$  they observed a broad enhancement in the two-jet mass spectrum in the neighbourhood of the W and Z masses which corresponded to a signal of  $632 \pm 190$

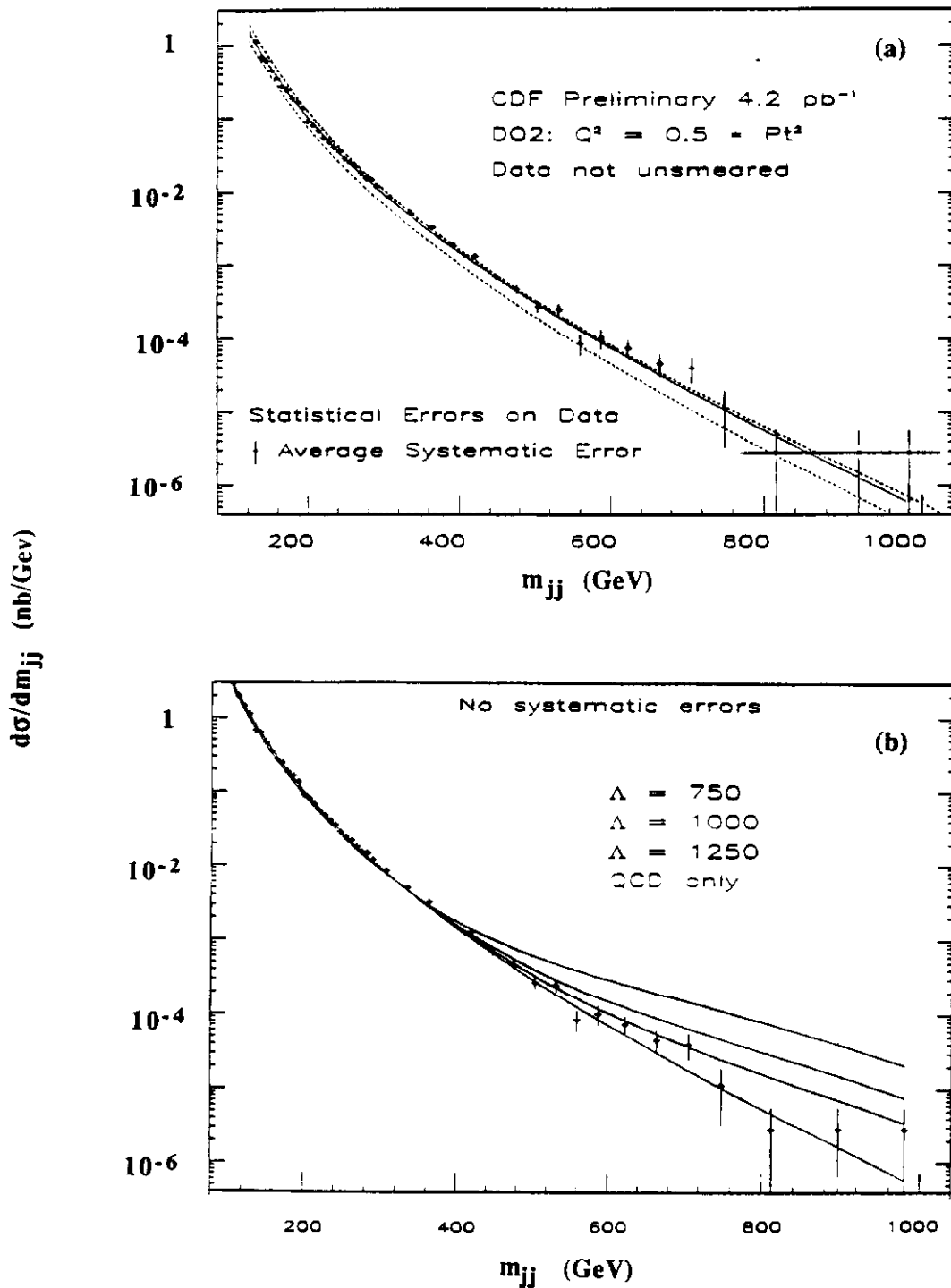


Fig. 3

Two-jet mass distribution: Preliminary CDF data (a) compared with leading order QCD predictions, where the broken lines show the uncertainty on the prediction arising from the choice of  $Q^2$  scale and structure function, and (b) compared with the expected deviations from QCD that would arise due to the presence of quark substructure at a scale  $\Lambda_C$ .

events. This was to be compared with the standard model expectation of  $340 \pm 80$  events passing their trigger and event selection.

The data from the 1989 CERN collider run increased the size of the UA2 data sample to  $4.7 \text{ pb}^{-1}$ . The two-jet mass distribution<sup>5</sup> in the neighbourhood of the Intermediate Vector Bosons is shown in figure 2 for events containing two well measured jets coplanar with the beam direction. There is a clear enhancement in the region of the W and Z boson masses. To extract the contribution to the mass spectrum from W and Z decays the spectrum has been fitted to two Gaussian peaks with the expected relative positions ( $m_Z/m_W = 1.14$ ) and the expected relative normalizations (corresponding to  $\sigma.B(Z \rightarrow q\bar{q})/\sigma.B(W \rightarrow q\bar{q}) = 0.43$ ) sitting on a background with the parameterized form  $m^{-\alpha}e^{-\beta m}e^{-\gamma m^2}$ . The W mass and the experimental mass resolution have been left as free parameters in the fit. The best fit gives  $m_W = 78.9 \pm 1.5 \text{ GeV}/c^2$  and a mass resolution of  $9.3 \pm 2.0 \%$ , both of which are consistent with expectations. The number of reconstructed events in the peak corresponds to a signal of  $5620 \pm 1130$  events (5 standard deviations) in agreement with the number which UA2 expected to pass their trigger and event selections based on standard model predictions ( $4250 \pm 150$  events).

In addition to being an important test of the standard model, the observation of W and Z decays to two hadronic jets is a reassuring confirmation of the relationship between the underlying partons and the reconstructed jets, and demonstrates the feasibility of jet spectroscopy at hadron colliders.

### 2.3 Two-jet Physics

Previous measurements of the two-jet differential cross section from the CERN experiments and the CDF experiment have extended up to two-jet masses of about  $300 \text{ GeV}/c^2$  and  $500 \text{ GeV}/c^2$  respectively<sup>6</sup> for jets produced centrally. The recent CDF data have enabled these measurements to be extended up to two-jet masses of about  $1000 \text{ GeV}/c^2$  (figure 3a). The preliminary measurements are in agreement with the lowest order QCD expectations.

A comparison of the measured differential two-jet cross section with the predictions of QCD can be used to search for quark substructure with an associated compositeness scale  $\Lambda_c$ . As the scale  $\Lambda_c$  is approached, quark substructure would be expected to give rise to an excess of jets with large  $p_T$ , and an excess of jet pairs emitted at large angle with respect to

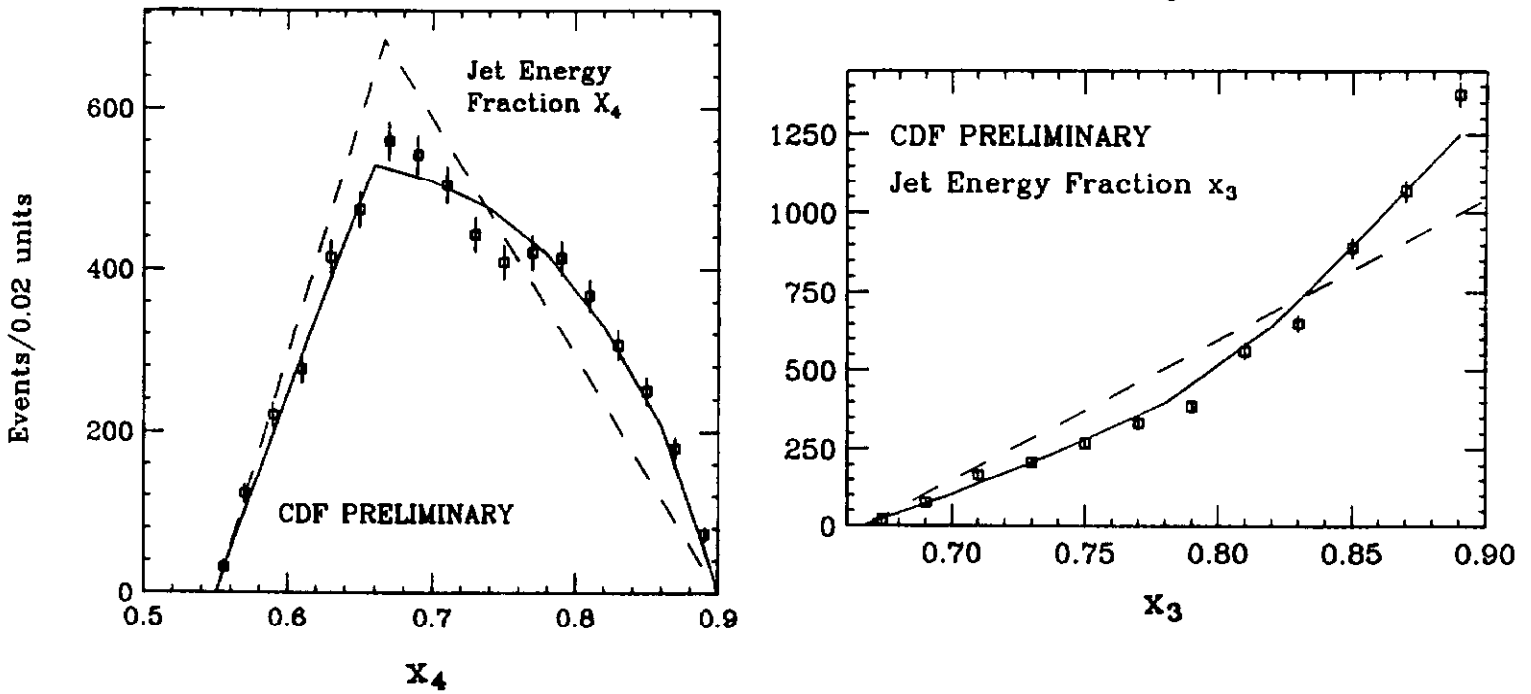


Fig. 4 Properties of three-jet events: Preliminary measured distributions from the CDF collaboration of the Dalitz plot variables  $X_3$  and  $X_4$  defined as the normalized energies of the highest energy and next to highest energy jets in the three-jet rest system. The  $X_i$  are normalized so that  $X_3 + X_4 + X_5 = 2$ . The solid curves show the leading order QCD predictions from the Papageno Monte Carlo. The broken curves show the predictions corresponding to three-body phase space.

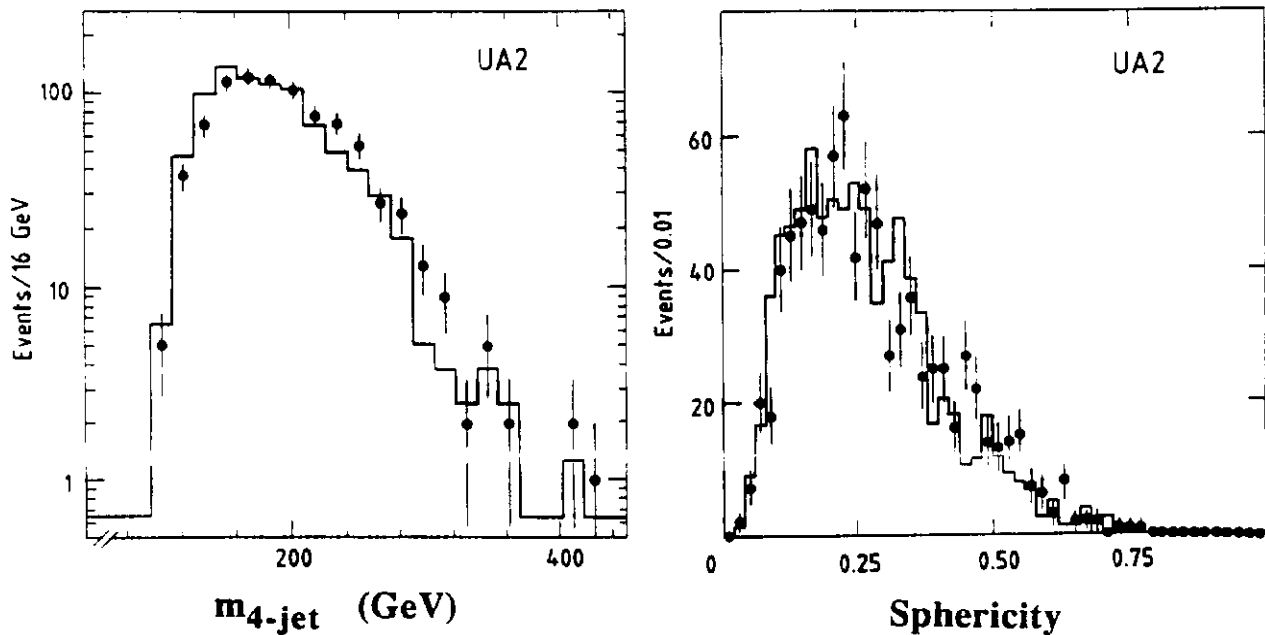


Fig. 5 Properties of four-jet events: Preliminary measured four-jet mass and event sphericity distributions for a sample of four-jet events. UA2 data<sup>5</sup> (points) are compared to the leading order QCD predictions of ref. 10 (histogram).

the beam direction and with large two-jet mass. Taking the form of the four fermion contact term to be given by <sup>7</sup> :

$$L_{\text{int}} = \frac{4\pi}{\Lambda_c^2} \bar{q}_L \gamma^\mu q_L \bar{q}_L \gamma_\mu q_L$$

the present lower limit on  $\Lambda_c$ , which comes from the absence of an excess of high  $p_T$  jets in the CDF inclusive differential jet spectrum<sup>8</sup>, is  $\Lambda_c > 0.95$  TeV at 90% confidence level. When the analysis of the 1988/9 CDF data is complete there should be a significant improvement in the sensitivity of the measurements to deviations from QCD expectations due to a finite  $\Lambda_c$ . An indication of the expected final sensitivity is shown in figure 3b which, for several choices of  $\Lambda_c$ , compares the preliminary two-jet mass spectrum with the expected deviations from the leading order QCD prediction.

## 2.4 Multi-Jet Production

The large increase in the sizes of jet data samples in the UA2 and CDF experiments enable detailed studies to be made of events containing three or more jets. In particular, preliminary measurements from the CDF experiment of the properties of three-jet events (figure 4) and from the UA2 experiment of the properties of four-jet events (figure 5) show<sup>5</sup> an impressive agreement with leading-order QCD predictions<sup>9,10</sup>. Events with five or more clearly separated jets have also been observed (figure 6) , offering an interesting test-bed for higher order QCD predictions. With the present data we can anticipate that in the coming months results should be forthcoming from the analysis of five-jet events, and maybe even six-jet events.

## 3. Direct Photons

A preliminary measurement of the inclusive differential cross-section for direct photon production from the 1988/9 CDF data<sup>11</sup> is shown in figure 7. The measured cross-section is a slightly steeper function of  $p_T$  than the current next-to-leading order QCD calculations<sup>12</sup> predict. It should be noted that the experimental photon isolation requirements are difficult to implement in a natural way in the  $O(\alpha_s^2)$  QCD calculation, which may account for the discrepancy between the QCD predictions and experimental observations at low  $p_T$ . The predictions give a good description of the data for photon transverse momenta in excess of 25 GeV/c. The new CDF measurements at  $\sqrt{s} = 1.8$  TeV complement the previous measurements of the UA1<sup>13</sup> and UA2<sup>14</sup> experiments at  $\sqrt{s} = 630$  GeV.



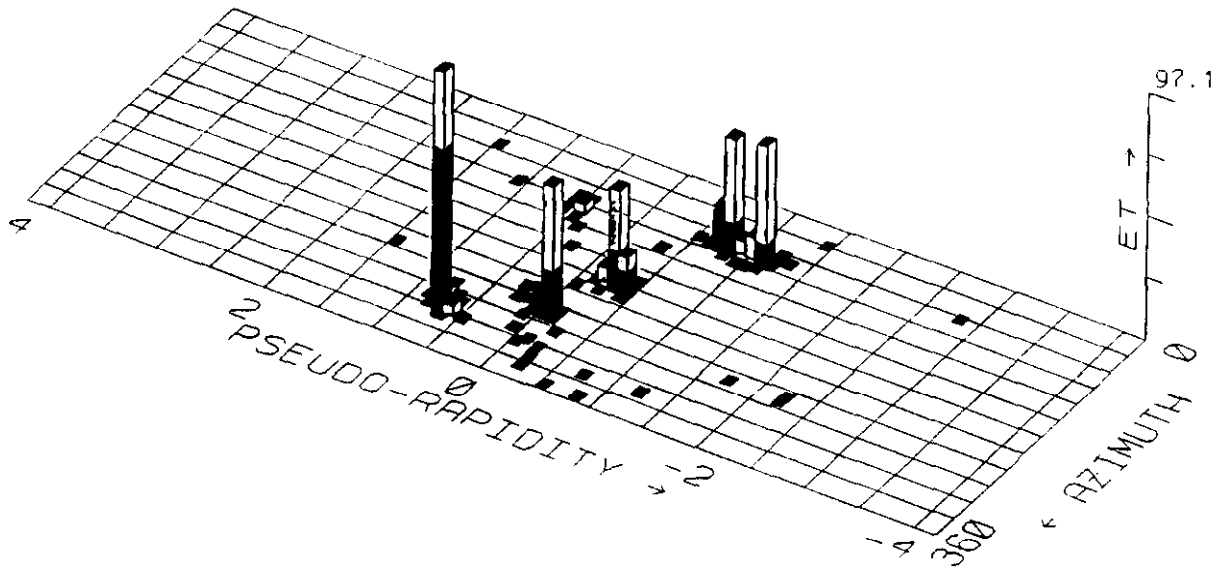


Fig. 6 Example of a five-jet event observed in the CDF experiment. The transverse energy flow is shown in the (pseudo-rapidity, azimuthal angle)-plane.

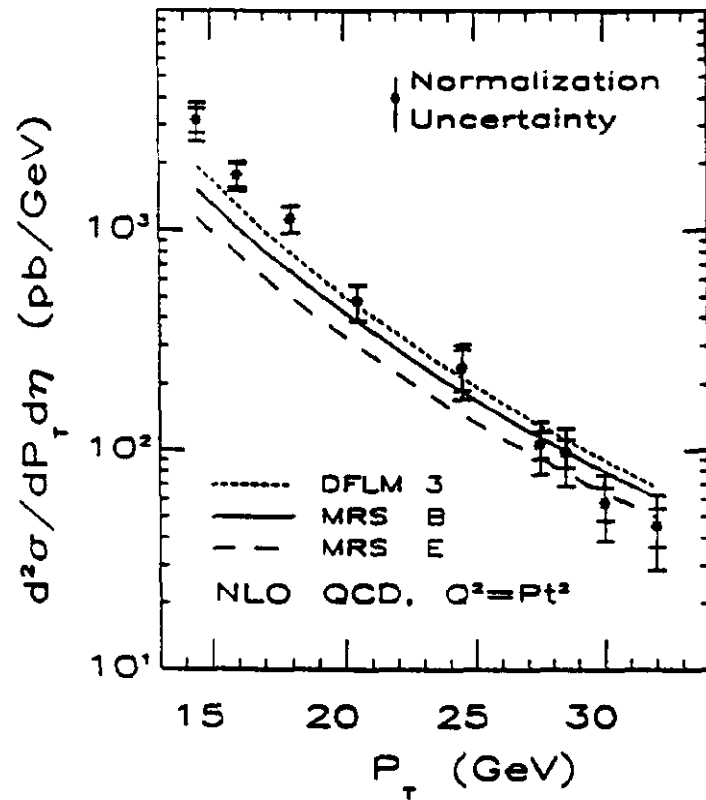


Fig. 7 Preliminary measurement of the inclusive direct photon cross-section from the CDF experiment. The curves show the next-to-leading order QCD predictions for a variety of structure functions.

## 4. W and Z Physics

Between them, during the 1988/9 running periods, the UA2 and CDF experiments have recorded of order 600 leptonic Z decays and 7000 leptonic W decays. These data samples have made possible improved measurements of the W and Z production rates, masses, and decay angular distributions, and searches for light Higgs bosons and exotic W and Z decays.

### 4.1 W and Z Masses

The W and Z masses measured by the proton-antiproton collider experiments are summarized in table 1. The Z mass results are in good agreement with those obtained at LEP and the SLC. Figure 8 compares the measurements in the  $m_W$  versus  $m_Z$  plane with standard model expectations as a function of the mass of the top quark and Higgs boson. The measured masses favor a top quark mass which is less than  $\sim 240 \text{ GeV}/c^2$ . The standard model expectations are not very sensitive to the assumed mass of the Higgs boson.

Defining the weak mixing angle  $\theta_W$  such that

$$\sin^2 \theta_W \equiv 1 - \frac{m_W^2}{m_Z^2}$$

the mass measurements imply:

$$\text{UA1}^{15}: \quad \sin^2 \theta_W = 0.211 \pm 0.025$$

$$\text{UA2}^{16}: \quad \sin^2 \theta_W = 0.2202 \pm 0.0084 \text{ (stat)} \pm 0.0045 \text{ (sys)}$$

$$\text{CDF}^{17}: \quad \sin^2 \theta_W = 0.231 \pm 0.012 \text{ (preliminary)}$$

in good agreement with the current world average value from deep inelastic scattering data:

$$\text{DIS}^{20}: \quad \sin^2 \theta_W = 0.2309 \pm 0.0029 \pm 0.0049.$$

### 4.2 W and Z Cross-Sections

In figure 9 the W and Z cross-sections times leptonic branching ratios measured both at CERN and Fermilab are shown to be in excellent agreement with the  $O(\alpha_S)$

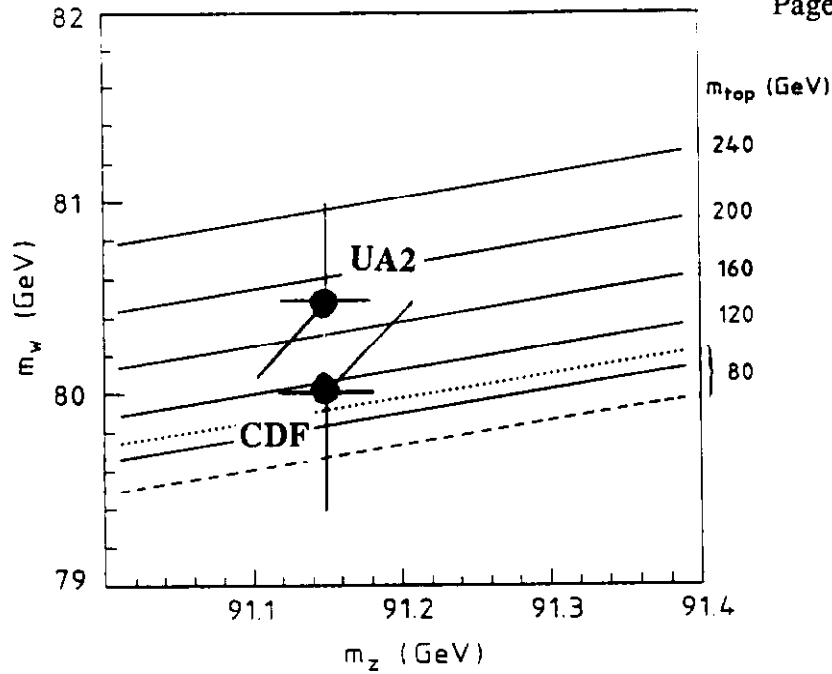


Fig. 8

Measured W and Z masses in the  $m_W$  versus  $m_Z$  plane compared with standard model expectations as a function of the mass of the top quark and Higgs boson. The solid lines correspond to a Higgs mass of  $100 \text{ GeV}/c^2$ . The dotted and dashed lines indicate the prediction for a top mass of  $80 \text{ GeV}/c^2$  with a Higgs mass of  $10 \text{ GeV}/c^2$  and  $1000 \text{ GeV}/c^2$  respectively. The position of the data points correspond to the measured Z mass from LEP and the measured W masses from UA2 and CDF.

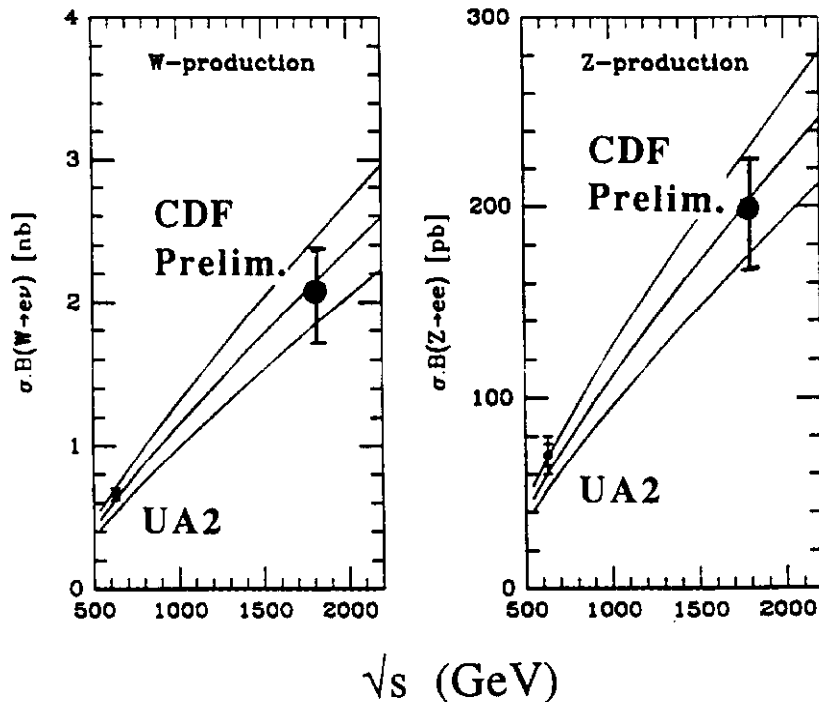


Fig. 9

Measured W and Z production cross-sections times leptonic branching ratios compared with standard model expectations. The band indicates the theoretical uncertainty on the predictions of ref. 21 arising from the uncertainty on the structure functions.

Table 1: W and Z masses.

Experiment	Channel	Mass (GeV/c <sup>2</sup> )	Width (GeV)
UA1 <sup>15</sup>	W → ev	m <sub>W</sub> = 82.7 ± 1.0 ± 2.7	
	W → μν	m <sub>W</sub> = 81.8 <sup>+6.0</sup> <sub>-5.3</sub> ± 2.7	
	W → τν	m <sub>W</sub> = 89.0 ± 3.0 ± 6.0	
UA2 <sup>16</sup>	W → ev	m <sub>W</sub> = 80.79 ± 0.31 ± 0.21 ± 0.81	1.89 <sup>+0.47</sup> <sub>-0.40</sub>
	W → ev	m <sub>W</sub> = 80.49 ± 0.43 ± 0.24 *)	
CDF <sup>17</sup>	W → ev	m <sub>W</sub> = 80.0 ± 0.2 ± 0.6 (preliminary)	
	W → μν	m <sub>W</sub> = 79.9 ± 0.4 ± 0.6 (preliminary)	
UA1 <sup>15</sup>	Z → e <sup>+</sup> e <sup>-</sup>	m <sub>Z</sub> = 93.1 ± 1.0 ± 3.0	
	Z → μ <sup>+</sup> μ <sup>-</sup>	m <sub>Z</sub> = 90.7 <sup>+5.2</sup> <sub>-4.8</sub> ± 3.2	
UA2 <sup>16</sup>	Z → e <sup>+</sup> e <sup>-</sup>	m <sub>Z</sub> = 91.49 ± 0.35 ± 0.12 ± 0.92	2.96 <sup>+0.98</sup> <sub>-0.78</sub>
CDF <sup>18</sup>	Z → e <sup>+</sup> e <sup>-</sup>	m <sub>Z</sub> = 91.5 ± 0.8 ± 0.4 (Tracking)	
	Z → e <sup>+</sup> e <sup>-</sup>	m <sub>Z</sub> = 91.1 ± 0.3 ± 0.4 (Calorimetry)	
	Z → μ <sup>+</sup> μ <sup>-</sup>	m <sub>Z</sub> = 90.7 ± 0.4 ± 0.2	
	Combined	m <sub>Z</sub> = 90.9 ± 0.3 ± 0.2	3.8 ± 0.8 ± 1.0
LEP <sup>19</sup>		m <sub>Z</sub> = 91.146 ± 0.033	2.540 ± 0.031

\*) Taking energy scale from LEP m<sub>Z</sub> measurements.

calculations of Altarelli et al.<sup>21</sup>. An interesting quantity is the ratio of cross-sections times branching ratios:

$$R \equiv \frac{\sigma_W \cdot B(W \rightarrow e\nu)}{\sigma_Z \cdot B(Z \rightarrow e^+e^-)} = \frac{\sigma_W}{\sigma_Z} \frac{\Gamma(W \rightarrow e\nu)}{\Gamma(Z \rightarrow e^+e^-)} \frac{\Gamma_Z}{\Gamma_W}$$

for which, within the standard model, the production cross-sections  $\sigma_W$  and  $\sigma_Z$ , and the partial widths  $\Gamma(W \rightarrow e\nu)$  and  $\Gamma(Z \rightarrow e^+e^-)$  can be calculated, and the total Z width  $\Gamma_Z$  taken from the LEP measurements. The ratio R is therefore sensitive to the total W width  $\Gamma_W$ . The measured values of R and the corresponding  $\Gamma_W$  are shown in table 2.

Table 2: Measured values of R and the corresponding W widths.

	R	$\Gamma_W$ (GeV)
UA2 <sup>22</sup> ( $\sqrt{s} = 630$ GeV)	9.38 <sup>+0.82</sup> <sub>-0.72</sub> ± 0.25	2.30 ± 0.19 ± 0.06
CDF <sup>23</sup> ( $\sqrt{s} = 1800$ GeV)	10.2 ± 0.8 ± 0.4	2.19 ± 0.20

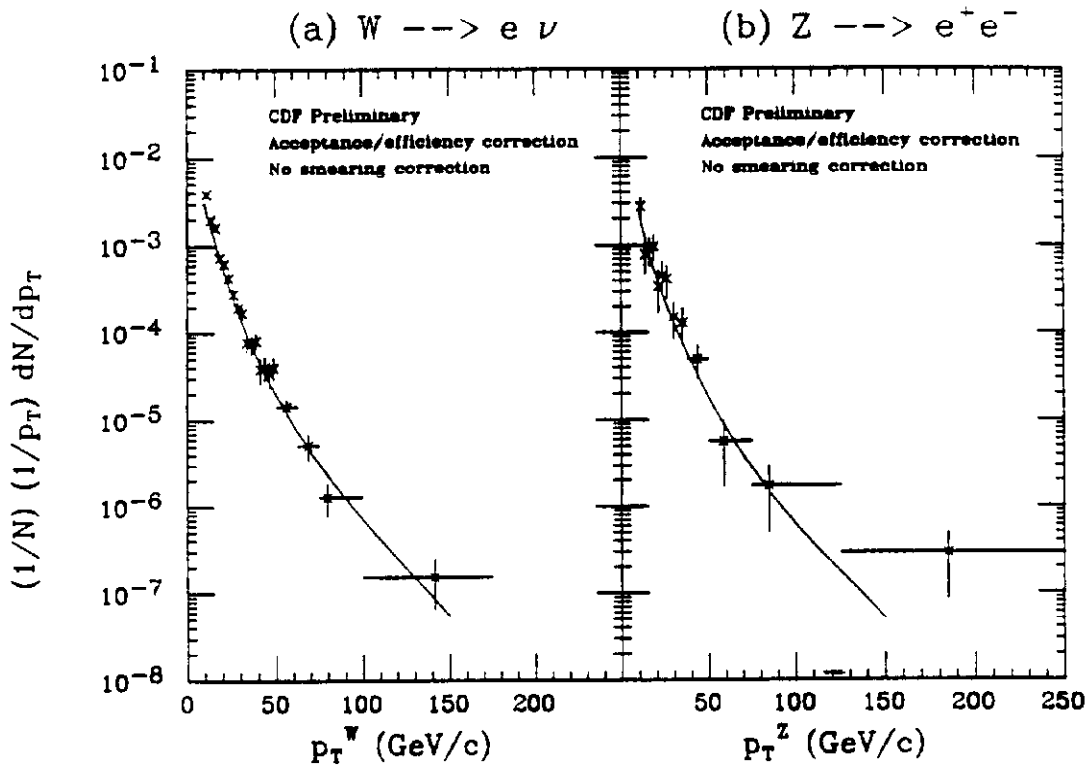


Fig. 10 Transverse momentum distributions of (a) W bosons and (b) Z bosons measured by the CDF collaboration, compared with the expectations from ref. [46] (curves).

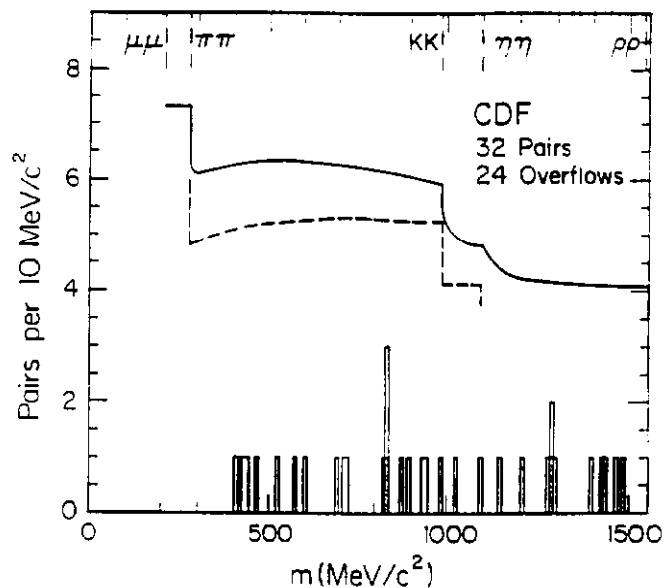


Fig. 11 Mass distribution of isolated high transverse momentum oppositely charged track pairs observed in W and Z events by the CDF collaboration. The average pair mass resolution is  $7 \text{ MeV}/c^2$ . The full line shows the expected contribution from a light standard model Higgs boson, and the dashed line indicates the theoretical floor for this prediction corresponding to the most pessimistic assumptions about the Higgs boson decay branching ratios.

These indirect measurements of the  $W$  width imply limits on the partial widths of  $W$  decays into  $t\bar{b}$  or more exotic decay modes. In particular the CDF measurement<sup>23</sup> implies that the top quark mass must be larger than  $41 \text{ GeV}/c^2$  at the 90% confidence level.

Finally, the differential cross-sections for  $W$  and  $Z$  production measured by UA2<sup>24</sup> and CDF<sup>25</sup> are in excellent agreement with the  $O(\alpha_s^2)$  expectations of Arnold and Reno<sup>26</sup>. The measurements from the CDF collaboration are shown in figure 10. No significant excess of events at high  $p_T$  is observed.

### 4.3 Search for a Light Higgs Boson

If a very light Standard Model Higgs boson exists with mass  $m_H < 1 \text{ GeV}/c^2$  then the radiation of a Higgs boson at the Fermilab collider is expected from about 1% of all hadronically produced  $W$  and  $Z$  bosons. If  $m_H$  is between the  $\mu^+\mu^-$  and  $\rho^+\rho^-$  decay thresholds ( $2m_\mu < m_H < 2m_\rho$ ) the Higgs boson is expected to (i) have a lifetime  $< 10^{-14}\text{s}$  and its decay products will therefore be associated to the primary vertex, and (ii) decay with a large branching fraction to a charged track pair ( $\mu^+\mu^-$ ,  $\pi^+\pi^-$ , or  $K^+K^-$ ). The CDF collaboration have therefore searched<sup>27</sup> for a resonant enhancement amongst isolated high-transverse-momentum track pairs in  $W$  and  $Z$  events. The pair mass distribution is shown in figure 11. No enhancement significantly in excess of statistical fluctuations is observed. Comparing the rate of isolated track pairs observed in  $W$  and  $Z$  events with the expectations for standard model Higgs boson production and decay, the mass intervals  $2m_\mu < m_H < 818 \text{ MeV}/c^2$ , and  $846 \text{ MeV}/c^2 < m_H < 2m_K$  are excluded at 90% C.L. This result is complementary to the recent negative results from light Higgs boson searches at  $e^+e^-$  colliders in that it is essentially based on the expected Higgs coupling to the  $W$  boson rather than the  $Z$  boson.

## 5. Heavy Flavor Physics

Heavy quarks (charm and bottom) are produced prolifically at hadron colliders. New preliminary results from the recent collider runs suggest that heavy flavor physics at hadron colliders has a rosy future. Results indicate the feasibility of reconstructing exclusive heavy quark decay modes which, combined with the expectation of very high statistics data samples in the near future, promises the possibility of (i) identifying exclusive final states for  $B_d$  and  $B_s$  mesons, (ii) measuring secondary vertices associated with the decays  $b \rightarrow c \rightarrow s$  and hence the associated  $B$  meson lifetimes, and (iii) studying  $B^0 - \bar{B}^0$  mixing as a

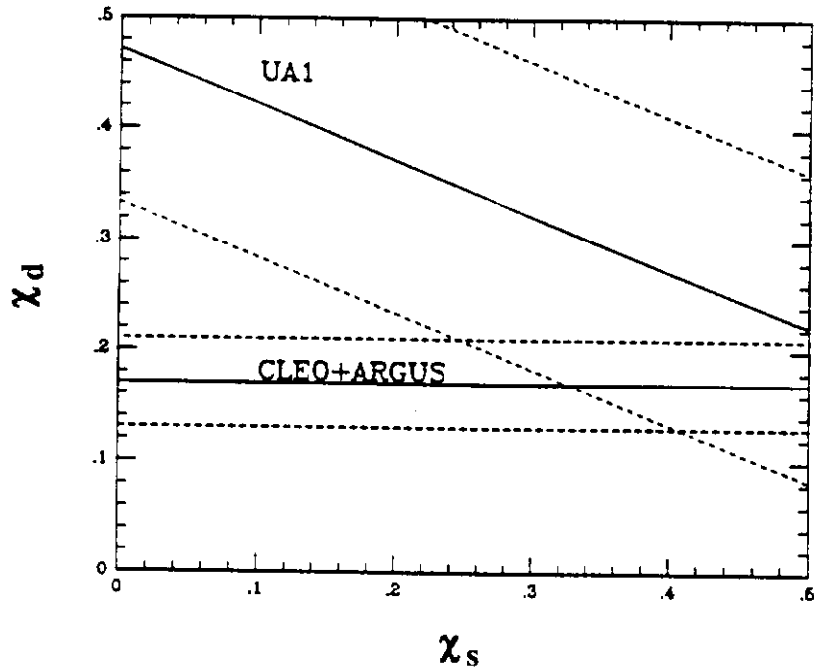


Fig. 12  $B^0 - \bar{B}^0$  mixing results from UA1, CLEO, and ARGUS. The bands indicated by the broken lines show the allowed region of the  $\chi_d$  versus  $\chi_s$  plane.

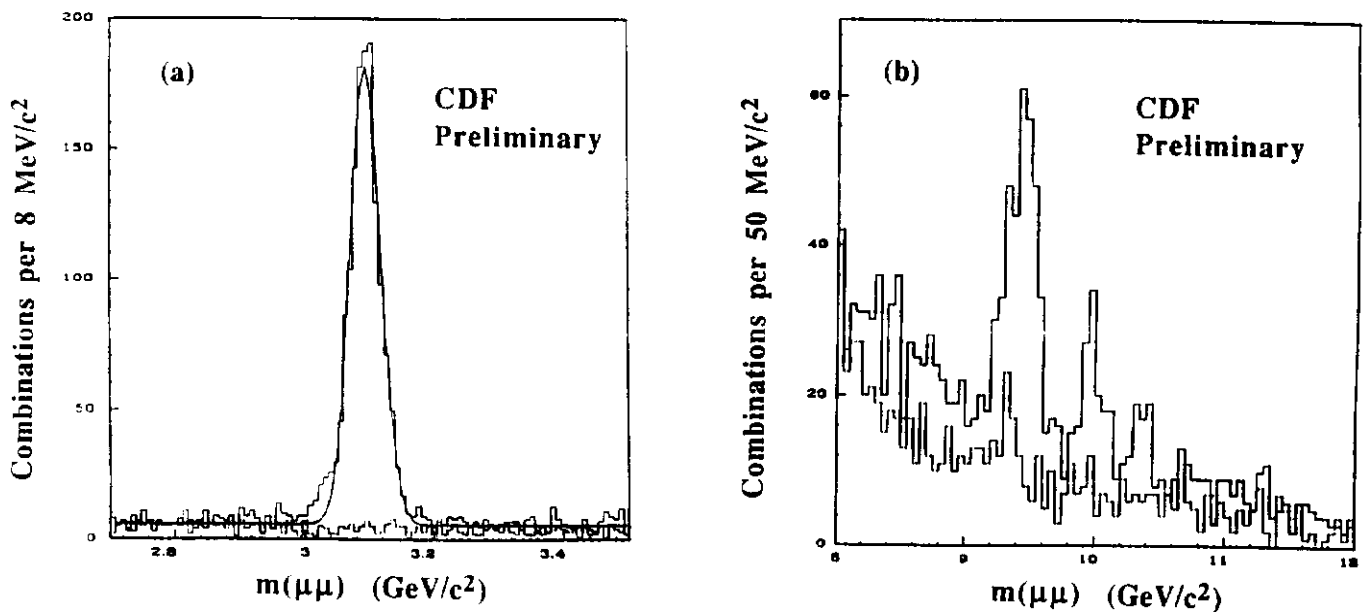


Fig. 13 Peaks observed in the  $\mu^+\mu^-$  spectrum by CDF. (a)  $J/\psi \rightarrow \mu^+\mu^-$  peak compared with a gaussian resolution function with a mass of  $3.0962 \text{ GeV}/c^2$  and a width of  $24.6 \text{ MeV}/c^2$ . (b)  $\Upsilon, \Upsilon', \text{ and } \Upsilon'' \rightarrow \mu^+\mu^-$  peaks.

function of decay length. In the more distant future with data samples of order  $1 \text{ fb}^{-1}$  searches for CP violation in the B meson system may be feasible.

### 5.1 $D^*$ s in Jets

Both the UA1 and CDF collaborations have measured  $D^{*\pm}$  production in jets produced in proton-antiproton collisions. The standard method is used to search for the decay sequence  $D^{*+} \rightarrow D^0 \pi_1^+$ ,  $D^0 \rightarrow K^- \pi_2^+$  (and its charge conjugate) by plotting the mass difference  $m(K^- \pi_1^+ \pi_2^+) - m(K^- \pi_2^+)$ . UA1 reports<sup>29</sup> a production rate of  $0.10 \pm 0.04 \pm 0.03$   $D^*$  mesons per jet for an average jet  $E_T$  of 41 GeV. This result is consistent with QCD expectations for production by gluon splitting. Furthermore the associated  $D^{*\pm}$  fragmentation distribution is strongly peaked towards  $z = 0$ , also consistent with a gluon splitting origin. The CDF measurements<sup>30</sup> at  $\sqrt{s} = 1.8 \text{ TeV}$  are in agreement with the UA1 measured  $D^{*\pm}$  rate at  $\sqrt{s} = 630 \text{ GeV}$ , the number of  $D^{*\pm}$  per jet observed by CDF is  $0.10 \pm 0.03 \pm 0.03$  for jets with an average  $E_T$  of 47 GeV.

### 5.2 $B^0 - \bar{B}^0$ mixing

The first evidence for  $B^0 - \bar{B}^0$  mixing<sup>31</sup> was from the UA1 measurement of like-sign dimuons produced in proton-antiproton collisions. The UA1 collaboration have recently updated their measurement. Defining the mixing parameter  $\chi$  as

$$\chi \equiv \frac{N(\bar{B}^0)}{N(B^0) + N(\bar{B}^0)}$$

where  $N(B^0)$  and  $N(\bar{B}^0)$  are the number of particles which decay as  $B^0$  mesons and  $\bar{B}^0$  mesons respectively given an initially pure beam of  $B^0$  mesons. UA1 measure<sup>32</sup>  $\chi = 0.18 \pm 0.08$  from their 1989 data, to be compared with  $0.16 \pm 0.06$  from their earlier (1983-1985) data. In principle there can be contributions to the production of like-sign dimuons from both  $B_d^0 - \bar{B}_d^0$  and  $B_s^0 - \bar{B}_s^0$  mixing, characterized by  $\chi_d$  and  $\chi_s$  respectively. To extract  $\chi_d$  and  $\chi_s$  requires knowledge of (i) the fraction of b quarks which hadronise as  $B_i^0$  mesons, (ii) the semi-muonic branching ratio of  $B_i^0$  mesons, and (iii) the average semi-muonic branching ratio for all bottom hadrons. Making reasonable assumptions for these parameters, and comparing with the results for  $B_d^0 - \bar{B}_d^0$  mixing from ARGUS<sup>33</sup> the UA1 collaboration concludes that both  $B_d^0 - \bar{B}_d^0$  and  $B_s^0 - \bar{B}_s^0$  mixing are needed to explain the data (figure 12).



### 5.3 Exclusive B Decays

Both UA1 and CDF have preliminary evidence for exclusive decay modes of B mesons. Firmer results from both experiments are expected in the near future. At present it is worth noting the impressive  $J/\psi$  and  $\Upsilon$ ,  $\Upsilon'$ , and  $\Upsilon''$  peaks reconstructed in the CDF detector (figure 13). Studies of exclusive B decays into  $J/\psi + X$  may yield interesting results in the coming years.

## 6. Search for the Top Quark

All three collider experiments have made direct searches for top quark production and decay. Since the purely hadronic decays of the top quark are difficult to separate experimentally from the much larger QCD multijet background, the experiments have focussed their searches on looking for semileptonic top decays. The absence of a signal enables limits to be placed on the production cross-section under the assumption that the semileptonic branching ratio  $BR(t \rightarrow \ell + X) = 11\%$ , as expected within the standard model. The  $O(\alpha_s^3)$  calculation<sup>28</sup> of the  $t\bar{t}$  production cross section in proton-antiproton collisions as a function of top quark mass, together with the predicted rate for  $W \rightarrow t\bar{b}$  events are shown in figure 14. Using these predictions the experimental limits on the top quark cross-sections can be converted into lower limits on the top quark mass. The current limits from UA1, UA2, and CDF are summarised in table 3.

### 6.1 Top Quark Limits from UA1

UA1 have looked for evidence for top quark production and semileptonic decay in the electron + jets channel (1983-1985 data<sup>34</sup>), muon + jets channel (1983-1989 data<sup>35</sup>), and di-muon channel (1983-1989 data<sup>35</sup>). Observed events are consistent with expectations for standard model background processes, e.g. W, Z, Drell-Yan, b-quark, and c-quark production. Limits on top quark production are obtained by constructing likelihood variables that differentiate between top decays and the various background processes.

### 6.2 Top Quark Limits from UA2

UA2 have looked for evidence for top quark production and semileptonic decay in the electron + jets channel<sup>36</sup>. The largest standard model background in this channel arises from W bosons produced in association with additional jet activity, where the W decays to

an electron and neutrino. The observed events have an electron-neutrino transverse mass distribution

$$m_T^{e\nu} \equiv (2p_T^e p_T^\nu [1 - \cos \phi_{e\nu}])^{1/2}$$

consistent with that expected for W production and decay without a contribution from the top quark. Fitting the  $m_T^{e\nu}$  distribution enables a limit on the top quark contribution to be placed as a function of the top quark mass, which in turn results in a limit on the top quark mass.

Table 3: Top quark mass limits from UA1, UA2, and CDF.

Experiment	Channel	Result (95% C.L.)
UA1 <sup>34,35</sup>	electron + $\geq 2$ jets	$m_t > 41 \text{ GeV}/c^2$
UA1 <sup>35</sup>	muon + $\geq 2$ jets	$m_t > 52 \text{ GeV}/c^2$
UA1 <sup>35</sup>	di-muon	$m_t > 46 \text{ GeV}/c^2$
UA1 <sup>35</sup>	combined	$m_t > 60 \text{ GeV}/c^2$
UA2 <sup>36</sup>	electron + jets	$m_t > 69 \text{ GeV}/c^2$
CDF <sup>37</sup>	electron + $\cancel{E}_T$ + $\geq 2$ jets	$m_t > 77 \text{ GeV}/c^2$
CDF <sup>38</sup>	electron + muon	$m_t > 72 \text{ GeV}/c^2$
CDF	combined including di-electron + $\cancel{E}_T$ , di-muon + $\cancel{E}_T$ , and Low $p_T$ muons	$m_t > 89 \text{ GeV}/c^2$ (preliminary)

### 6.3 Top Quark Limits from CDF

The most stringent limit on the top quark mass comes from the CDF experiment. Five complementary methods have been used to search for top quark semileptonic decays.

- (i) Electron +  $\cancel{E}_T$  +  $\geq 2$  jets<sup>37</sup>: the  $m_T^{e\nu}$  distribution is well described by expectations for  $W \rightarrow e\nu$  decays where the W is produced in association with hadronic jets. No excess ascribable to  $t\bar{t}$  or  $t\bar{b}$  production is observed.
- (ii) Electron + muon<sup>38</sup>: One event is observed with both an isolated electron and an isolated muon in the central region, both with  $p_T > 15 \text{ GeV}/c$ . This event has an electron with  $E_T = 31.7 \text{ GeV}$  and a muon with  $p_T = 42.5 \text{ GeV}/c$ . The dilepton azimuthal opening angle is  $137^\circ$ . There is also a second muon candidate in the event

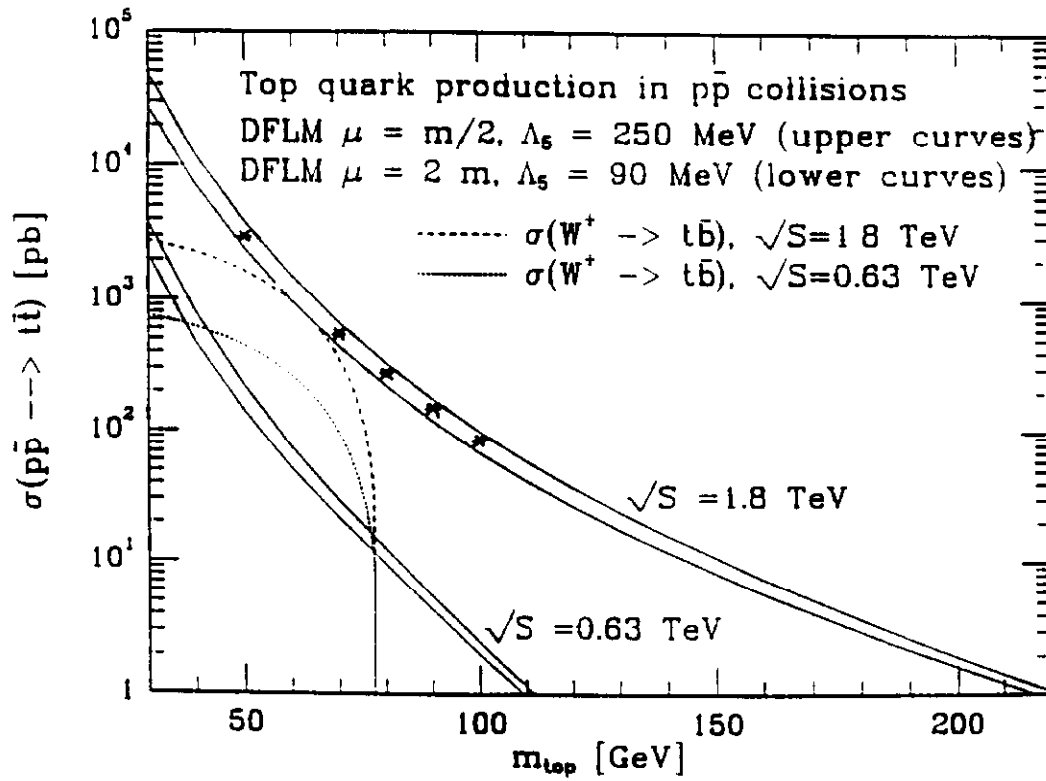


Fig. 14

Cross section for top quark production shown as a function of top quark mass.

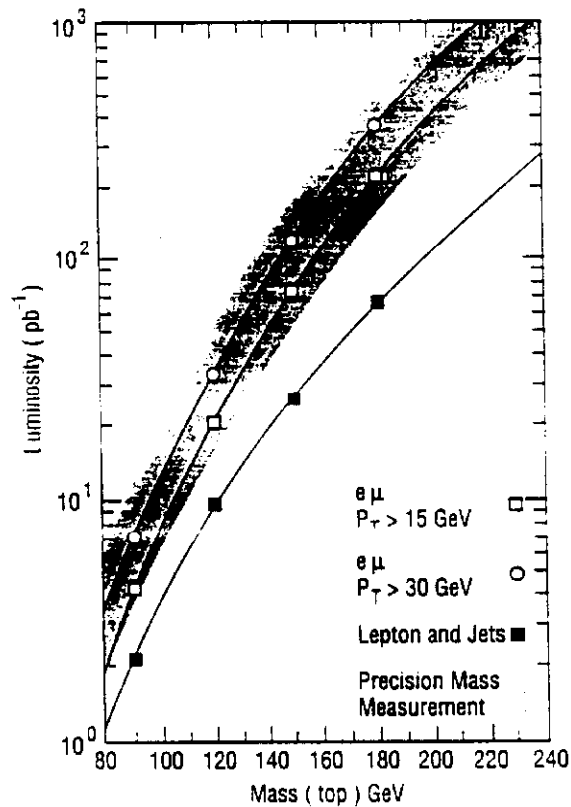


Fig. 15

Required luminosity to discover the top quark in proton-antiproton collisions at  $\sqrt{s} = 1.8$  TeV for various decay modes shown as a function of top quark mass.

in the forward region, and a jet with  $E_T = 14$  GeV. This event may be signal or may be background. For the purposes of extracting a conservative limit it is assumed to be signal. The limit on top quark production is then based on the observation of one event in the signal region.

- (iii) Di-electron +  $\cancel{E}_T$  [preliminary]: No events are observed with two isolated electrons with  $E_T > 15$  GeV,  $|m_{ee} - m_Z| > 15$  GeV/c<sup>2</sup>,  $\Delta E_T > 20$  GeV,  $\Delta\phi_{ee} > 20^\circ$ , and  $\Delta\phi_{ee} < 160^\circ$ .
- (iv) Di-muon +  $\cancel{E}_T$  [preliminary]: No events are observed with two isolated muons with  $E_T > 15$  GeV,  $|m_{\mu\mu} - m_Z| > 15$  GeV/c<sup>2</sup>,  $\Delta E_T > 20$  GeV,  $\Delta\phi_{\mu\mu} > 20^\circ$ , and  $\Delta\phi_{\mu\mu} < 160^\circ$ .
- (v) Low  $p_T$  muons [preliminary]: Look for additional low  $p_T$  muons in the electron +  $\cancel{E}_T + \geq 2$  jets sample and the muon +  $\cancel{E}_T + \geq 2$  jets sample, requiring the low  $p_T$  muon to be well separated from the highest  $p_T$  jets. No additional muons are observed far from the two highest  $E_T$  jets ( $\Delta R \equiv (\{\Delta\eta\}^2 + \{\Delta\phi\}^2)^{1/2} > 0.5$ ).

#### 6.4 Top Quark Status and Prospects

Currently the world data<sup>19,39</sup> suggest that the top quark has a mass in the approximate range 100 - 250 GeV/c<sup>2</sup>. The most stringent limit from direct searches for the top quark is  $m_t > 89$  GeV/c<sup>2</sup> (95% C.L.) from the CDF experiment. In 1991 the Fermilab collider is expected to begin its next run with CDF taking data and the D0 experiment having its first run. The integrated luminosity to be delivered by the collider will be about a factor of five more than during the 1988/9 run. The predicted  $t\bar{t}$  cross-section at the Fermilab collider is by about a factor of five lower for a top mass of  $\sim 125$  GeV/c<sup>2</sup> than for a mass of 89 GeV/c<sup>2</sup>, hence a first guess is that by 1992 the experiments should be sensitive to top decays if  $m_t < 125$  GeV/c<sup>2</sup>. This estimate is in fact over-conservative since top decays in the lepton + jets channel are more easily distinguished from the W + jets background as the top mass increases above the current limit. The results of a recent study<sup>40</sup>, which are shown in figure 15, suggest the experimental reach will approach  $m_t = 140$  GeV/c<sup>2</sup> by 1992, and  $m_t = 200$  GeV/c<sup>2</sup> by 1994 at which time the recorded integrated luminosity is expected to have increased by a further factor of five.

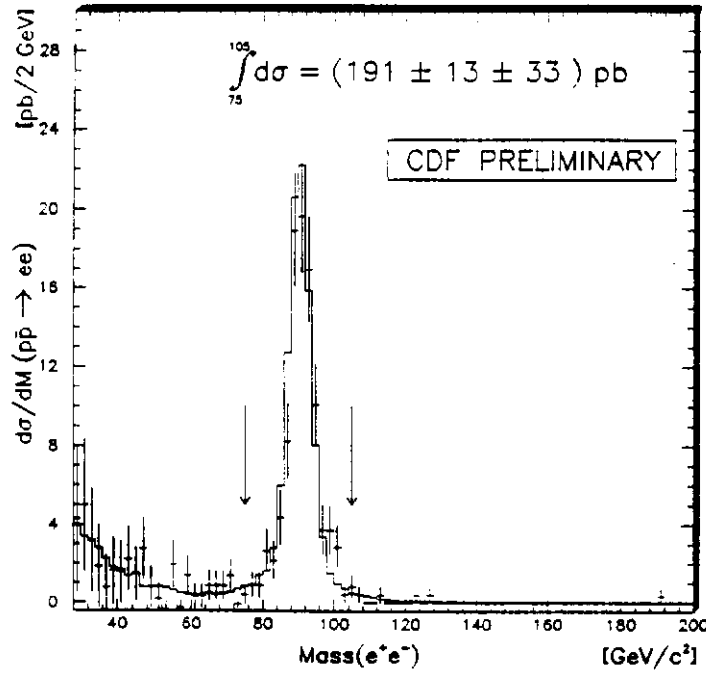


Fig. 16 Comparison of the  $e^+e^-$  mass distribution measured by the CDF collaboration with the standard model expectation (histogram).

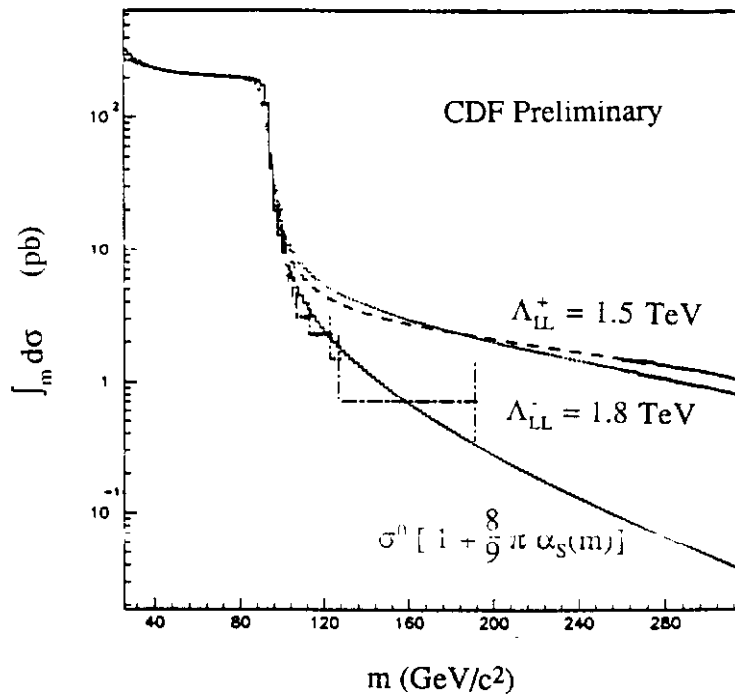


Fig. 17 Preliminary CDF measurement of the integrated  $e^+e^-$  cross-section compared with the  $O(\alpha_s)$  standard model expectation, and the modified expectations corresponding to an  $eeqq$  contact interaction with associated scales  $\Lambda_{LL}^+ = 1.5$  TeV and  $\Lambda_{LL}^- = 1.8$  TeV.

## 7. Search for Physics Beyond the Standard Model

Despite the large proton-antiproton collider data sets that have been recorded and analysed there are as yet no indications for a significant deviation from the expectations of the standard model. The agreement between measurements and predictions can be used to set limits on plausible modifications to the standard model. In the following the current status of searches for lepton compositeness, heavy W-like and Z-like bosons, and supersymmetric particles are summarised.

### 7.1 Lepton Compositeness

The  $e^+e^-$  pair differential cross-section measured by the CDF collaboration (figure 16) is well described by expectations for  $Z^0$  plus Drell-Yan production. No pair with mass in excess of  $200 \text{ GeV}/c^2$  is observed, corresponding to the preliminary upper limit :

$$\sigma_{e^+e^-}(m > 200 \text{ GeV}/c^2) < 2.1 \text{ pb (95\% C.L.)}.$$

This limit can be used to place a limit on the energy scale  $\Lambda_C$  associated with a flavor diagonal helicity conserving contact interaction of the form <sup>7</sup>:

$$\Lambda_C = \frac{\gamma^2}{2\Lambda^2} \eta_{LL} \hat{q}_L \gamma_\mu q_L \hat{e}_L \gamma_\mu e_L$$

with  $\eta_{LL} = \pm 1$ .

The resulting limits on  $\Lambda_C$  are:

$$\Lambda_{LL}^- > 1.8 \text{ TeV (95\% C.L.)},$$

$$\Lambda_{LL}^+ > 1.5 \text{ TeV (95\% C.L.)}.$$

Comparing the measured integral cross-section with  $O(\alpha\alpha_s)$  predictions (figure 17) it can be seen that these preliminary limits are conservative. More stringent limits should become available when the analysis is completed. Table 4 summarises the worlds limits on fermion compositeness scales. An analysis of the  $\mu^+\mu^-$  spectrum measured by CDF is currently in progress, and should yield a limit on (or observation of) a possible  $\mu\mu qq$  four fermion interaction in the near future.

Table 4: Lower limits on the scale of four fermion contact interactions.

	$\Lambda_{LL}^+$ (TeV)	$\Lambda_{LL}^-$ (TeV)	Experiment
$\Lambda_{LL}(eeee)$	1.4	3.3	TASSO <sup>41</sup>
$\Lambda_{LL}(ee\mu\mu)$	4.4	2.1	JADE <sup>42</sup>
$\Lambda_{LL}(ee\tau\tau)$	2.2	3.2	JADE <sup>42</sup>
$\Lambda_{LR}(\mu\nu_\mu e\nu_e)$	3.1 <sup>*</sup>	3.1 <sup>*</sup>	Jodidio et al. <sup>43</sup>
$\Lambda_{LL}(qqqq)$	0.95	0.95	CDF <sup>8</sup>
$\Lambda_{LL}(eeqq)$	1.5	1.8	CDF (Preliminary)

\*) 90% C.L.

## 7.2 Search for a Heavy W and Z Bosons

The most stringent limits on the production and leptonic decay of high mass W-like and Z-like bosons come from the CDF data. No additional peaks are observed in the  $e^+e^-$  mass spectrum above the  $Z^0$ , or in the  $e\nu$  transverse mass distribution above the W, which are ascribable to the decays of heavy  $W'$  or  $Z'$  bosons. The resulting 95% C.L. upper limits on the production at  $\sqrt{s} = 1.8$  TeV times leptonic decay branching ratios are:

$$\sigma_{W'} \cdot B_{e\nu} \leq 7.6 \text{ pb}$$

and

$$\sigma_{Z'} \cdot B_{ee} \leq 1.0 \text{ pb.}$$

These limits can be re-expressed as limits on the  $W'$  and  $Z'$  masses if standard model couplings are assumed:

$$m_{W'} > 380 \text{ GeV}/c^2 \text{ (95\% C.L.)},$$

and

$$m_{Z'} > 400 \text{ GeV}/c^2 \text{ (95\% C.L.)}.$$

### 7.3 Squarks and Gluinos

CDF has searched for events containing two or more hadronic jets produced in association with large missing transverse energy ( $\cancel{E}_T$ ). There are 98 events with  $\cancel{E}_T > 40$  GeV. The observed  $\cancel{E}_T$  spectrum is shown in figure 18. The expected background contributions have been calculated for  $W \rightarrow e\nu$ ,  $W \rightarrow \mu\nu$ ,  $W \rightarrow \tau\nu$ ,  $Z \rightarrow \nu\bar{\nu}$  and QCD multijet events including the contribution from the production and decay of heavy quarks. The total expected background ( $86.4 \pm 14.1 \pm 11.6$  events from Intermediate Vector Boson decay, and  $4 \pm 4$  events from QCD) is consistent with the observed event rate. Using the ISAJET Monte Carlo together with a simulation of the CDF detector, the non-observation of an excess of multijet plus large  $\cancel{E}_T$  events can be used to place limits on the masses of squarks and gluinos. Assuming (i) the photino is the lightest supersymmetric particle and is massless, (ii) that there are six degenerate squark masses, and (iii) that the SUSY quantum number is conserved, the resulting region of the squark mass versus gluino mass plane that is excluded is shown in figure 19. A search has also been made by CDF for two photons produced in association with large  $\cancel{E}_T$ . Events of this type are predicted by models in which the photino is unstable and the Higgsino is the lightest supersymmetric particle. Preliminary mass limits on squarks and gluinos from this search<sup>44</sup> are similar to those shown in figure 19.

### 7.4 Selectrons, Sneutrinos, Winos, and Photinos

The UA2 collaboration have searched for supersymmetric decays of the  $Z^0$  in the channels:

$$Z \rightarrow \tilde{e}\tilde{e} \rightarrow ee\tilde{\gamma}\tilde{\gamma}$$

and

$$Z \rightarrow \tilde{\omega}\tilde{\omega} \rightarrow ee\tilde{\nu}\tilde{\nu}.$$

These decays result in a relatively low mass  $e^+e^-$  pair produced together with  $\cancel{E}_T$ . UA2 do not see any evidence for an excess of such events that can be ascribed to these decay modes<sup>45</sup>. Limits on supersymmetric decays are obtained by dividing the kinematic space into 19 regions and fitting for standard model plus SUSY contributions. The resulting excluded regions in the  $m_{\tilde{e}}$  versus  $m_{\tilde{\gamma}}$  and  $m_{\tilde{\omega}}$  versus  $m_{\tilde{\nu}}$  planes are shown in figure 20.



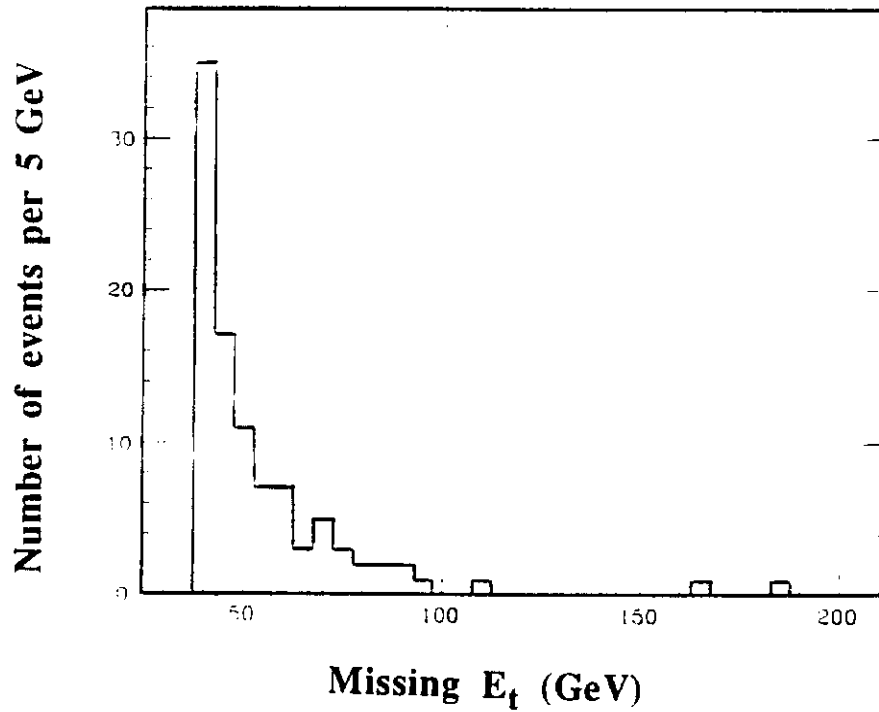


Fig. 18 Distribution of  $\cancel{E}_T$  observed by the CDF collaboration for events with  $\cancel{E}_T > 40$  GeV and two or more hadronic jets.

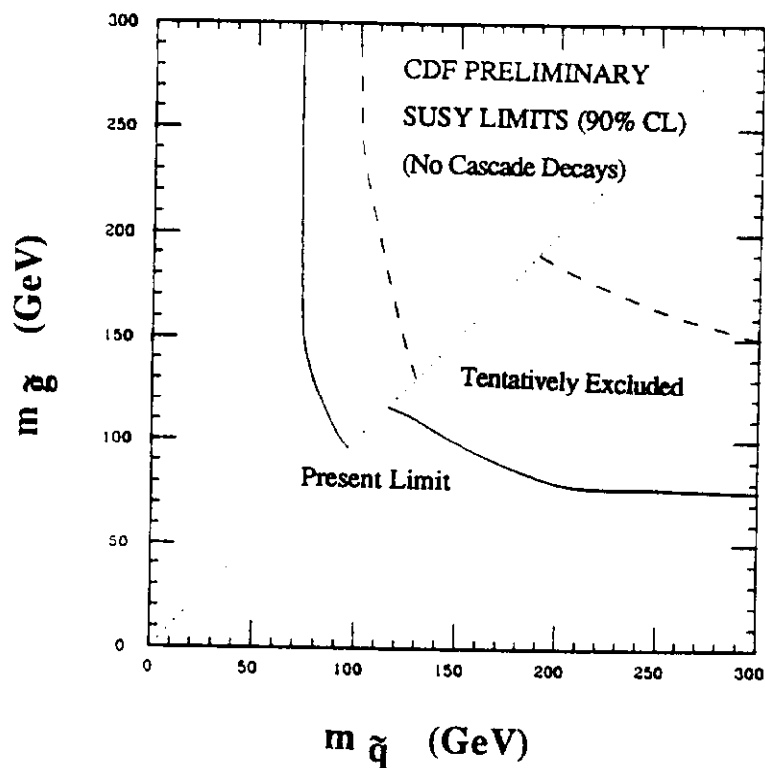


Fig. 19 Regions of the squark versus gluino mass plane excluded (90% C.L.) by the CDF collaboration for a minimal SUSY model where the photino is the lightest supersymmetric particle and is massless and stable.

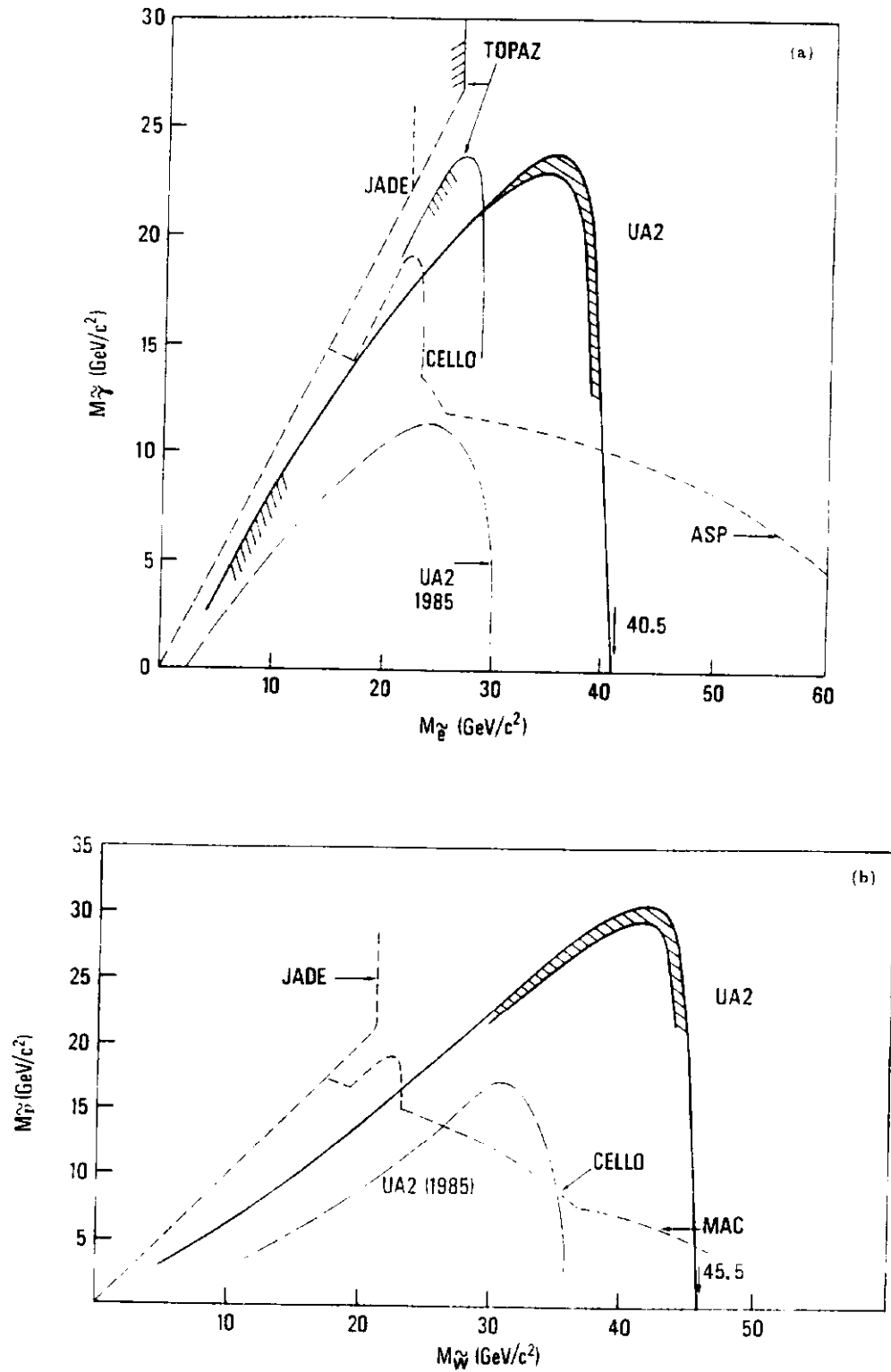


Fig. 20

Excluded regions from the UA2 experiment at the 90% C.L. in (a) the  $(m_{\tilde{e}}, m_{\tilde{\nu}})$  plane, and (b) the  $(m_{\tilde{u}}, m_{\tilde{\nu}})$  plane. The dashed area indicates the effect of systematic uncertainties

## 8. Summary

The large increases in the data samples recorded at the CERN and Fermilab high energy proton-antiproton colliders in the last two years have made possible many new results in jet physics, direct photon measurements, electroweak tests, and searches for new particles.

The main jet physics results have been the new preliminary measurements of the inclusive jet, two-jet, three-jet, and four-jet cross-sections and the confirmation of the earlier UA2 observation of the decay of the W and Z into two jets. In particular the first comparison of the inclusive jet cross-section measured by CDF with the complete next-to-leading order QCD predictions has been made, and promises in the future a substantial improvement in the precision of the comparison between QCD and the measurements. In the domain of direct photon physics further work is needed to understand the apparent discrepancy between predictions and measurements of the direct photon cross-section at low photon  $p_T$ . The main W and Z physics results have been the increasingly precise measurements of the W and Z masses and widths. The W width has been measured both by direct fitting of the lepton transverse mass distributions, and indirectly from the measured relative rates of leptonic W and Z decays.

Searches have been made for additional heavy W-like and Z-like bosons, fermion substructure, supersymmetric particles and a light Higgs boson. No evidence for any of these phenomena has been reported. There is as yet no statistically significant evidence for the top quark. If it should turn out that the one electron-muon candidate observed by CDF does indeed come from  $t\bar{t}$  production and decay then the next few years of proton-antiproton collider physics should be exciting ones.

## 9. References

- [1] S. D. Ellis, Z. Kunst. and D. Soper, Phys. Rev. Lett. 62 (1989) 726.
- [2] F. Aversa et al., presented at the 8th Topical Workshop on Proton-Antiproton Collider Physics, Castiglione della Pescaia, Sept. 1989; CERN-TH-5710/90 (1990).
- [3] R. K. Ellis and J. C. Sexton, Nucl. Phys. B282 (1987) 642.
- [4] R. Ansari et al. (UA2 Collab.) Phys. Lett. 186B (1987) 452.
- [5] K. Meier (UA2 Collab), presented at the 8th Topical Workshop on Proton Antiproton Collider Physics, Castiglione della Pescaia, Italy, Sept. 1989, CERN-EP/89-178.

- [6] F. Abe et al. (CDF Collab.) Phys. Rev. D41 (1990) 1722.
- [7] E. Eichten et al., Phys. Rev. Lett. 50 (1983) 811.
- [8] M. Dell'Orso (CDF Collab.), Proc. Les Rencontres de Physique de la Vallée D'Aosta, La Thuile, Italy, March 1990.
- [9] F. Berends et al., Phys. Lett. 103B (1981) 124.
- [10] Z. Kunst and W.J. Stirling, Phys. Lett. 171B (1986) 307.
- [11] R. Harris (CDF Collab.), to be published in the proceedings of the Workshop on Hadron Structure Functions and Parton Distributions, Fermilab, April 1990; CDF/PUB/JET/PUBLIC/1210.
- [12] P. Aurenche, R. Baier, and M. Fontannaz, FERMILAB-PUB-89/226-T (1989).
- [13] C. Albajar et al. (UA1 Collab.), Phys. Lett. 209B (1988) 385.
- [14] R. Ansari et al. (UA2 Collab.), Z. Phys. C41 (1989) 395.
- [15] C. Albajar et al. (UA1 Collab.), submitted to Z. Phys. C, CERN-EP/88-168 (1988).
- [16] J. Alitti et al. (UA2 Collab.), submitted to Phys. Lett., B, CERN-EP/90-22 (1990).
- [17] W. Trischuk (CDF Collab.), Thesis, Harvard University (1990).
- [18] F. Abe et al. (CDF Collab.), Phys. Rev. Lett. 63 (1989) 720.
- [19] A. Blondel, submitted to Phys. Lett. B, CERN-EP/90-10 (1990).
- [20] G.L. Fogli and D. Haidt, Z. Phys. C40 (1988) 379.
- [21] G. Altarelli et al., Nucl. Phys. B157 (1979) 461; B246 (1984) 12; Z. Phys. C27 (1985) 617.
- [22] J. Alitti et al. (UA2 Collab.), submitted to Z. Phys. C, CERN-EP/90-20.
- [23] F. Abe et al. (CDF Collab.) Phys. Rev. Lett. 64 (1990) 152.
- [24] D. Wood (UA2 Collab.) presented at the 8th Topical Workshop on Proton-Antiproton Interactions, Castiglione della Pescaia, Italy, Sept. 1989.
- [25] T. Kamon (CDF Collab.) presented at the 8th Topical Workshop on Proton-Antiproton Interactions, Castiglione della Pescaia, Italy, Sept. 1989.
- [26] P. Arnold and M.H. Reno, Nucl. Phys. B319 (1989) 37, and erratum Fermilab PUB 89/59-T (1989).
- [27] F. Abe et al. (CDF Collab.), Phys. Rev. D41 (1990) 1717.
- [28] P. Nason, S. Dawson, and R.K. Ellis, Nucl. Phys. B303 (1988) 607.
- [29] C. Albajar et al. (UA1 Collab.), submitted to Phys. Lett. B, CERN-EP/90-61 (1990).
- [30] F. Abe et al. (CDF Collab.), Phys. Rev. Lett. 64 (1989) 348.
- [31] C. Albajar et al. (UA1 Collab.), Phys. Lett. B186 (1987) 247.

- [32] N. Ellis (UA1 Collab.), presented at the 8th Topical Workshop on Proton-Antiproton Collider Physics, Castiglione della Pescaia, Sept. 1989.
- [33] H. Albrecht et al. (ARGUS Collab.), Phys. Lett. B192 (1987) 245.
- [34] C. Albajar et al. (UA1 Collab.), Z. Phys. C37 (1988) 505.
- [35] C. Albajar et al. (UA1 Collab.), submitted to Zeitschrift fur Physik C, CERN-EP/90-57 (1990).
- [36] T. Akesson et al. (UA2 Collab.), submitted to Zeitschrift fur Physik C, CERN-EP/89-152 (1989).
- [37] F. Abe et al. (CDF Collab.), Phys. Rev. Lett. 64 (1990) 142.
- [38] F. Abe et al. (CDF Collab.), Phys. Rev. Lett. 64 (1990) 147.
- [39] J. Ellis and G.L. Fogli, Phys. Lett. B232 (1989) 139.  
P. Langacker, Phys. Rev. Lett. 63 (1989) 1920.  
W.A. Bardeen, C.T. Hill, and M. Lindner, Phys. Rev. D41 (1990) 1647.  
G. Buchalla, A.J. Buras, and M.K. Harlander, MPI-PAE/PTh 63/89 (1989).  
F. Halzen and D.A. Morris, Phys. Lett. B237 (1990) 107.
- [40] S. Abachi et al., presented at "physics at Fermilab in the 1990s", Breckenridge, CO, August 1989.
- [41] Braunsch et al. (TASSO Collab.), Z. Phys. C37 (1988) 171.
- [42] Bartel et al. (JADE Collab.), Z. Phys. C31 (1986) 359.
- [43] Jodidio et al., Phys. Rev. D34 (1986) 1967; D37 (1986) 237.
- [44] S. Mikamo (CDF Collab.), presented at the 8th Topical Workshop on Proton-Antiproton Collider Physics, Castiglione della Pescaia, Italy, Sept. 1989.
- [45] T. Akesson et al. (UA2 Collab.), submitted to Phys. Lett., CERN-EP/89-172 (1989).
- [46] A.C. Bawa and W.J. Stirling, Phys. Lett. B203 (1988) 172.